Materials Science and Technology

ISSN: 0267-0836 (Print) 1743-2847 (Online) Journal homepage: https://www.tandfonline.com/loi/ymst20

Comparative study of fracture toughness of austempered ductile irons with upper and lower ausferrite microstructures

P. Prasad Rao & S. K. Putatunda

To cite this article: P. Prasad Rao & S. K. Putatunda (1998) Comparative study of fracture toughness of austempered ductile irons with upper and lower ausferrite microstructures, Materials Science and Technology, 14:12, 1257-1265, DOI: 10.1179/mst.1998.14.12.1257

To link to this article: https://doi.org/10.1179/mst.1998.14.12.1257

Published online: 19 Jul 2013.

Comparative study of fracture toughness of austempered ductile irons with upper and lower ausferrite microstructures

P. Prasad Rao and S. K. Putatunda

A ductile iron was austempered at 302 and 385°C for various times to get lower and upper ausferrite microstructures respectively. The microstructures were characterised by optical microscopy and X-ray diffraction. Plane strain fracture toughness was determined under all heat treatment conditions. While the austempered ductile iron with lower ausferrite microstructure showed higher fracture toughness, the one with upper ausferrite microstructure exhibited higher tensile toughness and strain hardening coefficient. A model was developed relating fracture toughness to the yield strength (σ_y) volume fraction of retained austenite (X_γ) and the carbon content of the retained austenite (C_γ). Experimental results showed excellent agreement with the prediction of the model that K_{IC}^2 is proportional to $\sigma_y(X_\gamma C_\gamma)^{1/2}$. *MST/3897*

At the time the work was carried out, the authors were in the Department of Chemical Engineering and Materials Science, College of Engineering, Wayne State University, Detroit, MI, USA. Professor Prasad Rao is now in the Department of Metallurgical and Materials Engineering, Karnataka Regional Engineering College, Surathkal, Karnataka, India. *Manuscript received 12 August 1997; in final form 28 January 1998.*

Introduction

Austempered ductile cast iron (ADI) is a very attractive material for many engineering applications because of its excellent combination of high strength and ductility.[1–7] It also exhibits good wear resistance[8–10] and fatigue strength.[11–13] It is expected that it will replace forged steel in many applications, especially in the automobile industry. The remarkable properties of ADI are attributed[1–4] to its unique microstructure of ferrite and austenite rather than ferrite and carbide as in austempered steels. Because of this difference in microstructure, the product of austempering treatment in ductile iron is referred to as ausferrite rather than bainite. By controlling the austempering time and temperature, the relative proportions of ferrite and austenite as well as the fineness of the ferrite can be varied over a wide range. This results in considerable variation in mechanical properties.

Fracture toughness, which is a measure of a material's resistance to crack growth under sustained monotonic loading conditions, is an extremely important parameter for structural design. Structural components designed on the basis of fracture toughness are not expected to fail in service. Investigations have shown that ADI possesses good fracture toughness comparable with heat treated low alloy steels.[14–17] A good understanding of the influence of microstructure on fracture toughness of ADI is necessary in order to optimise the heat treatment parameters. Several investigators[18–23] have studied the influence of heat treatment parameters on the fracture toughness of ADI. Bartosiewicz *et al.*[18] studied the fracture toughness of two alloyed ductile irons austempered at four different temperatures and found that fracture toughness is a function of the volume fraction of ferrite and retained austenite. Fracture toughness peaked at a retained austenite content of 30 vol.-% in the matrix. They therefore concluded that for optimum fracture toughness ADI should be austempered at 280°C. Putatunda and Singh[19] found that a peak in fracture toughness of unalloyed ADI was obtained when the matrix had ~22 vol.-% of retained austenite. They suggested that, in specimens with larger volume fractions of retained austenite, carbon content may be non-uniform because of long diffusion distances. In such cases, regions with lower carbon may be unstable and transform to martensite during crack propagation, causing lower fracture toughness. However, these specimens exhibited higher tensile toughness. Doong *et al.*[20] also examined the influence of austempering temperature on the fracture toughness of ADI. Austempered ductile iron with a lower ausferrite microstructure was found to exhibit better fracture toughness than ADI with an upper ausferrite microstructure. However, specimens austempered at 400°C had only 5 vol.-% of retained austenite while those austempered at 450°C had none. This suggests that the specimens had been austempered for too long at these temperatures, so that the second stage of the austempering reaction had set in. Poor fracture toughness in these cases may therefore be due to extensive carbide precipitation. Doong and Chen[21] also showed that ADI with a lower ausferrite microstructure had better fracture toughness than ADI with upper ausferrite. They concluded that the optimum austempering temperature is between 300 and 350°C.

Thus it is generally observed that fracture toughness initially increases with increasing austempering temperature, reaches a maximum value and then decreases with further rise in temperature. The maximum fracture toughness is observed at ~300°C. An ADI with a lower ausferrite microstructure generally has better fracture toughness than one with an upper ausferrite microstructure. While the retained austenite content had been estimated in all the studies discussed above, no attempt had been made to correlate it with fracture toughness. The carbon content of the retained austenite is an equally important parameter, yet apparently no work had been done on its relation to fracture toughness. Nor had any quantitative correlation between the fracture toughness and these microstructural parameters been developed. The present work was therefore undertaken to address these issues, and to develop a model relating the fracture toughness and microstructural parameters.

Experimental work

The chemical composition of the ADI used in the present work was Fe–3·5C–2·65Si–0·4Mn–0·01S–0·021P–0·035Mg–0·55Cu–1·6Ni–0·3Mo (wt-%). Cylindrical tensile specimens and compact tension specimens machined from cast slabs were austenitised at 871°C for 2 h. These were subsequently austempered at 302°C and 385°C for 15 min, 30 min,

60 min, 90 min, and 2 h. The austempering temperatures were so selected that 302°C was expected to give a lower ausferrite microstructure, while 385°C was expected to give an upper ausferrite microstructure. Different austempering times were selected so as to get a variation in the amount of retained austenite at each temperature.

The microstructures of the heat treated specimens were studied by optical microscopy after etching with 2% nital. The volume fraction of retained austenite and its carbon content in all the specimens were estimated by X-ray diffraction using the technique of Rundman and Klug.[24] X-ray diffraction profiles were obtained on a Rigaku rotating head anode diffractometer at 40 kV and 100 mA using crystal monochromated Co $K_{\alpha 1}$ radiation. The specimens were scanned in the angular 2θ ranges of 42–46° and 70–105°. The profiles were computer analysed to obtain the peak positions as well as the integrated intensities. The volume fraction of the retained austenite X_γ was determined by the direct comparison method[25] using integrated intensities of the (110) and (211) peaks of ferrite, and the (111), (220), and (311) peaks of austenite. The carbon content of the austenite was determined using the relationship[26]

$$a_\gamma = 0{\cdot}3548 + 0{\cdot}0044C_\gamma \quad \ldots\ldots\ldots\ldots \quad (1)$$

where a_γ is the lattice parameter of austenite in nanometres and C_γ is its carbon content (wt-%). The (111), (220), and (311) peaks of austenite were used to estimate the lattice parameter.

Tensile tests were carried out according to ASTM Standard E–8 (Ref. 27) at a constant engineering strain rate of $4 \times 10^{-4}\,s^{-1}$ on an MTS 810 servohydraulic machine. Specimen dimensions are shown in Fig. 1*a*. Three specimens were tested in each case and the values reported are an average of these. Fracture toughness testing was carried out according to ASTM Standard E–399 (Ref. 28), and also on an MTS 810 servohydraulic machine. Dimensions of the compact tension specimens are shown in Fig. 1*b*. Five identical specimens were tested for each heat treatment condition. Values reported are averages of these five tests. Fracture surfaces of the tensile specimens as well as the fracture toughness specimens were examined on a Hitachi S–2400 scanning electron microscope.

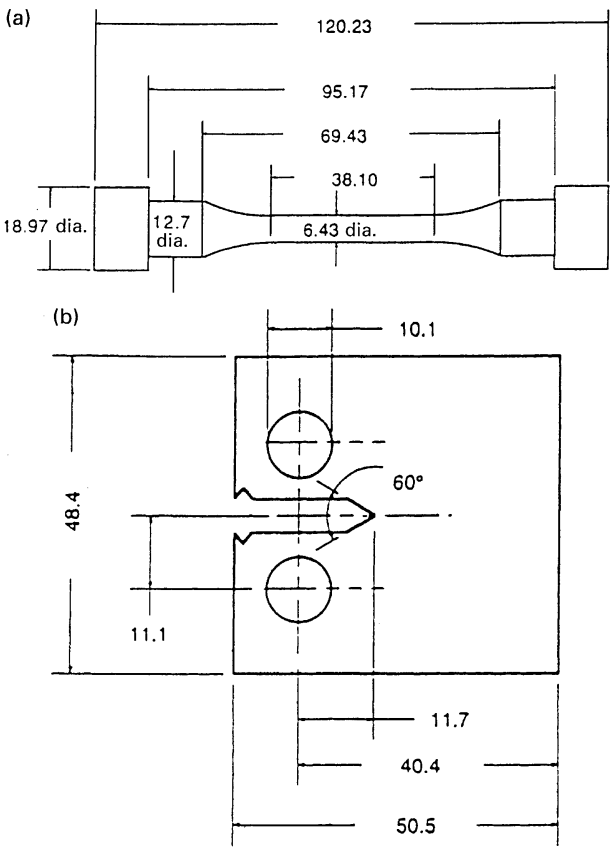

a tensile; *b* compact tension

1 Schematic diagram of test specimens: dimensions in millimetres

Results and discussion

MICROSTRUCTURE

There are significant differences between austempering reactions in ductile iron and in steel. When steel is austempered, the resulting microstructure consists of a fine dispersion of carbides in a ferritic matrix. However, in ductile iron, the presence of a large amount of silicon suppresses the carbide formation. When ferrite forms within the austenite the carbon ejected from these regions goes into solution in the surrounding austenite. As more and more ferrite forms the carbon content of the austenite increases. Since this high carbon austenite is stable at room temperature, the resulting microstructure consists of ferrite and retained austenite. This is the desired microstructure. However, if the specimen is held for too long at the austempering temperature, the austenite may decompose into ferrite and carbide, which is not desirable because of the embrittling effect of the carbide. Therefore, the microstructure of an ADI depends on the austempering temperature and time. The important microstructural features are the morphology of the ferrite, the retained austenite content, the carbon content of the retained austenite, and the presence or absence of carbide in the austenite or ferrite.

The specimens austempered for different times at the two temperatures in the present work were studied by optical microscopy to establish the morphology of ferrite. X-ray diffraction analysis was carried out to ascertain the amount of retained austenite and its carbon content.

Optical microscopy

Some typical microstructures are shown in Fig. 2. Specimens austempered at 302°C showed acicular ferrite characteristic of the lower ausferrite microstructure, while those austempered at 385°C showed the broad feathery type of ferrite characteristic of upper ausferrite microstructure. Specimens austempered for only 15 min, at both temperatures, showed incomplete transformation, evidenced by regions free of ferrite in the intercellular regions. Unstabilised austenite which exists in these regions transforms to martensite on quenching.

X-ray diffraction

The volume fraction of retained austenite and its carbon content, as estimated by X-ray diffraction, are shown in Fig. 3*a* and *b*. The retained austenite is found to increase with increasing austempering time at both temperatures, and reach a saturation value after about 60 min. While the maximum amount of retained austenite was 39 vol.-% at 385°C, it was only about 26 vol.-% at 302°C. At the higher austempering temperature the diffusion of carbon from regions transforming into ferrite to the surrounding austenite is greater than at the lower temperature. Thus at a given austempering time, there is more retained austenite at the higher temperature.

At the austempering temperature of 302°C, the carbon content of the austenite rose gradually from a low value of 1·04 wt-% at 15 min to 1·7 wt-% at 90 min and remained practically constant thereafter. However, at 385°C, the carbon content was found to be high at 1·63 wt-% even after only 15 min; it rose only gradually with increasing

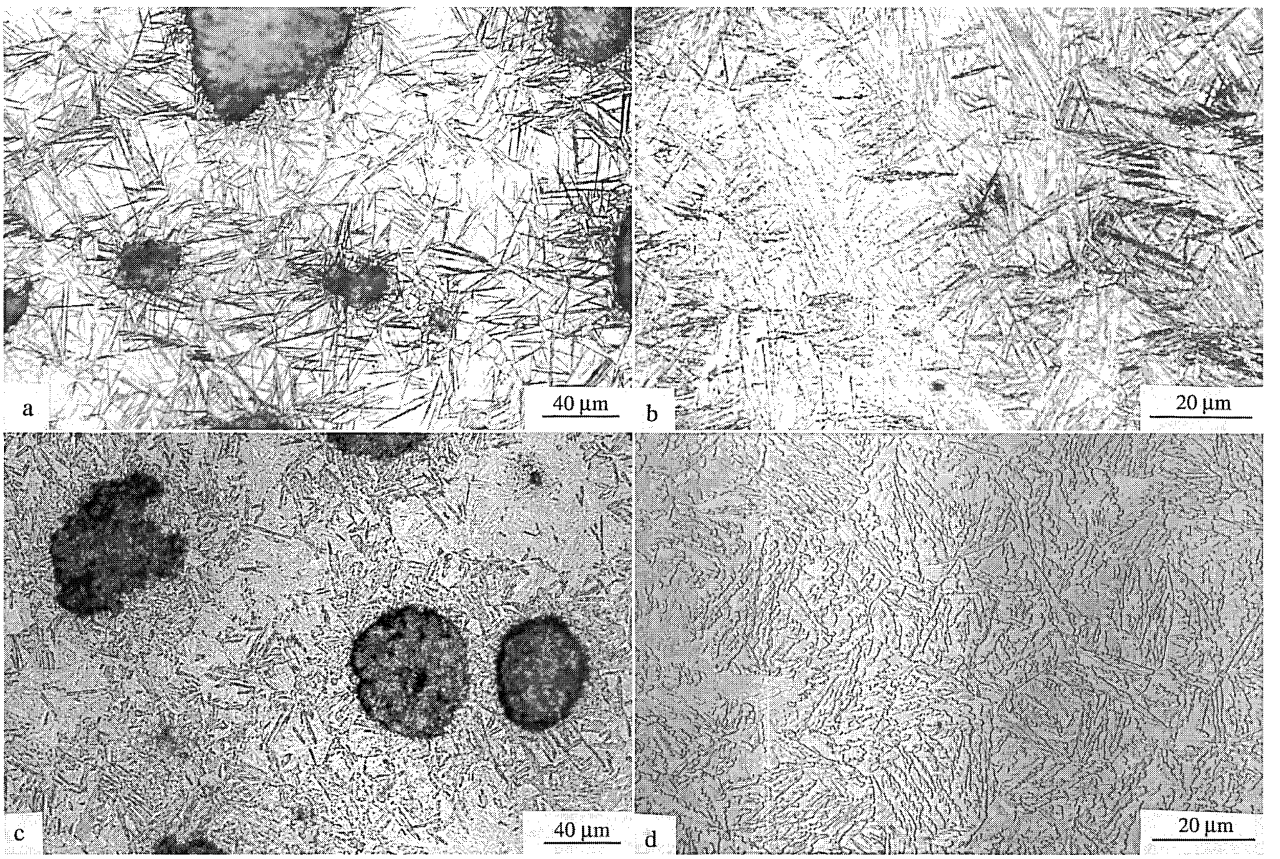

a 302°C for 15 min; *b* 302°C for 90 min; *c* 385°C for 15 min; *d* 385°C for 90 min

2 Microstructures of austempered specimens

austempering time. Beyond 60 min a gradual drop was observed which suggested that the second stage of the austempering process had been initiated, where the austenite decomposes into ferrite and carbide. The X-ray diffraction profiles, however, did not show any peaks corresponding to the carbide. This may be because either the amount of carbide is too small to give any appreciable intensity to its peaks, or, since the two strongest peaks of carbide are very close to the (111) peak of austenite and the (110) peak of ferrite, they may have merged.

The maximum carbon contents of ~1·7 wt-% at 302°C and 385°C in retained austenite reported in the present investigation are lower than the values often reported in the literature.[29] The lower carbon content in the present work is because of the higher amount of retained austenite in the present specimens, which is caused by the higher alloy content. When ferrite forms at the higher austenitising temperatures, all the carbon in the region that transformed to ferrite is ejected into the surrounding austenite. At the end of the stage I reaction, therefore, the retained austenite of the ausferrite will contain all the carbon in the original austenite. The total carbon in the retained austenite is given by the parameter $X_\gamma C_\gamma$, which is 0·64 for a specimen austempered at 385°C. The carbon

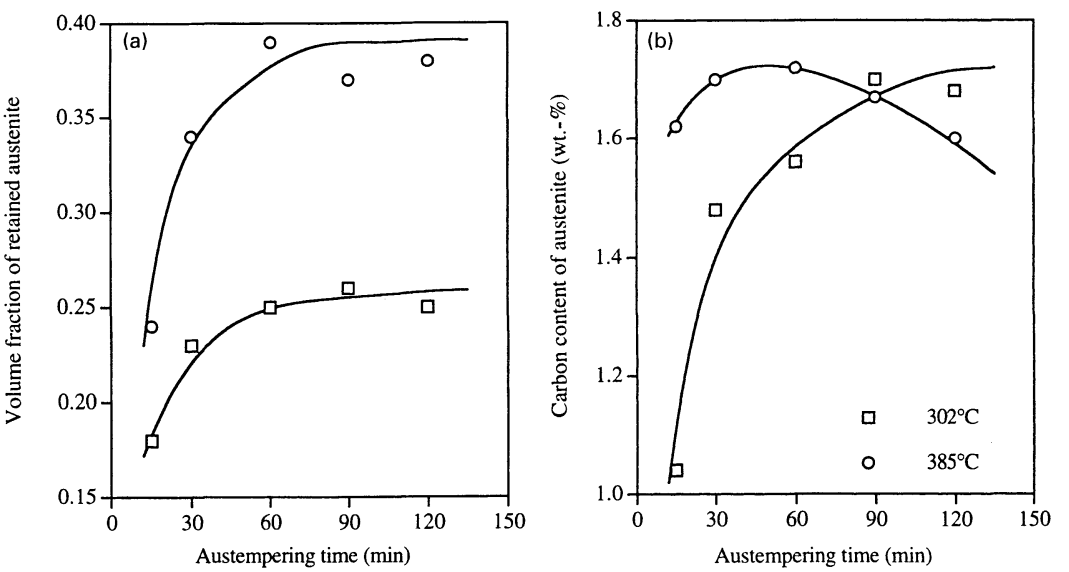

3 Variation of *a* volume fraction and *b* carbon content of retained austenite with austempering time

content of the original austenite can be estimated from the following relationship[30]

$$C_0 = (T_\gamma/420) - 0{\cdot}17[\mathrm{Si}] - 0{\cdot}95 \quad . \quad . \quad . \quad . \quad . \quad . \quad . \quad (2)$$

where C_0 is the carbon content (wt-%), T_γ the austenitising temperature in °C, and [Si] is weight per cent silicon in the iron. Under the present conditions this works out to be 0·67 wt-%. Thus, nearly all this carbon is found in the retained austenite. When austempered at the lower temperature of 302°C, the total carbon in the retained austenite is found to be only 0·44 wt-%, showing that a significant amount of carbon is present in the ferrite, probably as carbides. The results of the present investigation correlate well with those of Rouns and Rundman.[29] They have studied the microstructures of several ductile irons subjected to different austempering treatments in detail. Their results show that increasing alloy content increases X_γ and decreases C_γ. For an unalloyed ductile iron austenitised at 871°C and austempered at 371°C, the retained austenite and its carbon content were reported as 26 vol.-% and 1·98 wt-% respectively, while for an alloyed ductile iron containing 1·5 wt-%Ni and 0·3 wt-%Mo, these were 34 vol.-% and 1·87 wt-% respectively. Since the present ductile iron has a high alloy content, X_γ is high at 44 vol.-%, while C_γ is relatively low at 1·63 wt-%. The parameter $X_\gamma C_\gamma$ is a better indicator of the carbon content of the retained austenite.

TENSILE PROPERTIES

The variation of yield strength, tensile strength, and percentage elongation with austempering time at the two temperatures is shown in Fig. 4*a–c*. The lower austempering temperature gave much higher strength values than the higher temperature. For specimens treated at 302°C the ductility is low and does not vary much with time. But for the specimens treated at 385°C, it is very sensitive to austempering time, rising from a low 2% at 15 min to a high value of 10% at 2 h. The tensile properties can be directly correlated with the microstructure. The acicular ferritic structure resulting from the low austempering temperature leads to higher strength. However at this temperature, the small variation in austenite content with austempering time (Fig. 3*a*), results in a small variation in ductility. When austempered at 385°C, the austenite content shows a large increase with austempering time which in turn leads to a large increase in ductility. This high austenite content and the broad feathery needles of ferrite characteristic of upper ausferrite give high ductility and tensile toughness, while the low austenite content and fine acicular ferrite characteristic of lower ausferrite results in much lower tensile toughness.

Tensile toughness was estimated for all heat treatment conditions using the relationship[31]

$$\text{tensile toughness} = \frac{\sigma_y + \sigma_u}{2}\varepsilon_f \quad . \quad . \quad . \quad . \quad . \quad . \quad . \quad . \quad (3)$$

where σ_y and σ_u are the yield strength and tensile strength respectively, while ε_f is the fracture strain. The estimated values are reported in Table 1. It can be seen that at all

Table 1 Tensile toughness (MPa) of specimens after austempering for given times at temperatures of 302 and 385°C

Time, min	302°C	385°C
15	30·01	17·58
30	34·15	43·20
60	51·02	78·30
90	50·14	74·80
120	46·29	76·10

austempering times, except at 15 min, specimens austempered at 385°C have better tensile toughness than those austempered at 302°C. It was also found that specimens austempered at 385°C had higher strain hardening coefficients than those austempered at 302°C. The strain hardening coefficient was estimated using the Hollomon[32] relationship

$$\sigma = k\varepsilon^n \quad . \quad . \quad . \quad . \quad . \quad . \quad . \quad . \quad . \quad . \quad . \quad . \quad . \quad . \quad . \quad (4)$$

where σ is the true flow stress, ε is true strain, n is the strain hardening coefficient and k is the constant of proportionality. A plot of ln σ agianst ln ε yielded a straight line as shown in Fig. 4*d* for the specimens austempered for 60 min at the two temperatures. The strain hardening coefficient n, which is the slope of the straight line, was estimated as 0·09 at 302°C and 0·21 at 385°C. There was no significant variation in n with austempering time. The higher austenite content and higher carbon content of the retained austenite at the higher austempering temperature results in higher strain hardening capability.

FRACTURE TOUGHNESS

Fracture toughness values after austempering for different durations at the two austempering temperatures are presented in Fig. 4*e*. When austempered at 302°C the fracture toughness increased rapidly from 15 to 60 min, and then remained nearly constant beyond that. The fracture toughness values are comparable to those of hardened and tempered low alloy steels. At the higher temperature of 385°C, fracture toughness increased gradually from 15 to 90 min, and then decreased with further increase in time. The results clearly show that an ADI with a lower ausferrite microstructure has superior fracture toughness to an ADI with an upper ausferrite microstructure. The former also has much higher strength than the latter. Thus we have a material with higher strength and higher fracture toughness.

We can now estimate the defect tolerance of the material. For an infinite plate containing a sharp crack of length $2a$, the critical value of fracture toughness K_{1C} is given as[31]

$$K_{1C} = \sigma Y(\pi a_c)^{1/2} \quad . \quad . \quad . \quad . \quad . \quad . \quad . \quad . \quad . \quad . \quad . \quad . \quad (5)$$

where Y is equal to unity. Nominal applied stress σ depends on the appropriate design code. Here, a value of half the yield strength is assumed for illustrative purposes. Figure 4*f* shows the critical crack length a_c values at different austempering times for the two austempering temperatures. Most of these are longer than 3 mm and therefore are easily detectable by conventional NDT techniques. From the fracture design point of view ADI can easily be used for structural applications. As in Fig. 4*e*, the 385°C plot reaches a peak, while the 302°C plot rises with increasing time until 60 min and remains nearly constant beyond that. However, now the curve at 385°C is above the curve 302°C. This should not be taken as indicating higher fracture toughness of the ADI with upper ausferrite structure. The critical defect size is larger only because the nominal stress is lower. For example, if the specimen austempered at 302°C for 60 min is stressed to 306 MPa, as was the specimen austempered for 60 min at 385°C (*see* Fig. 4*f*), the critical crack length is 12·9 mm, more than twice the critical crack length of the upper ausferrite structure.

Fractographic studies were carried out on the fracture toughness specimens. These are shown in Figs. 5 and 6 for specimens austempered at 302°C and 385°C. When austempered for a short time (15 min), an intergranular cleavage fracture was observed at both temperatures (Figs. 5*a* and 6*a*). With short periods of austempering some martensite is formed in the intercellular regions, as noted above. This brittle phase provides the preferential path for the propagation of cleavage fracture. These specimens had

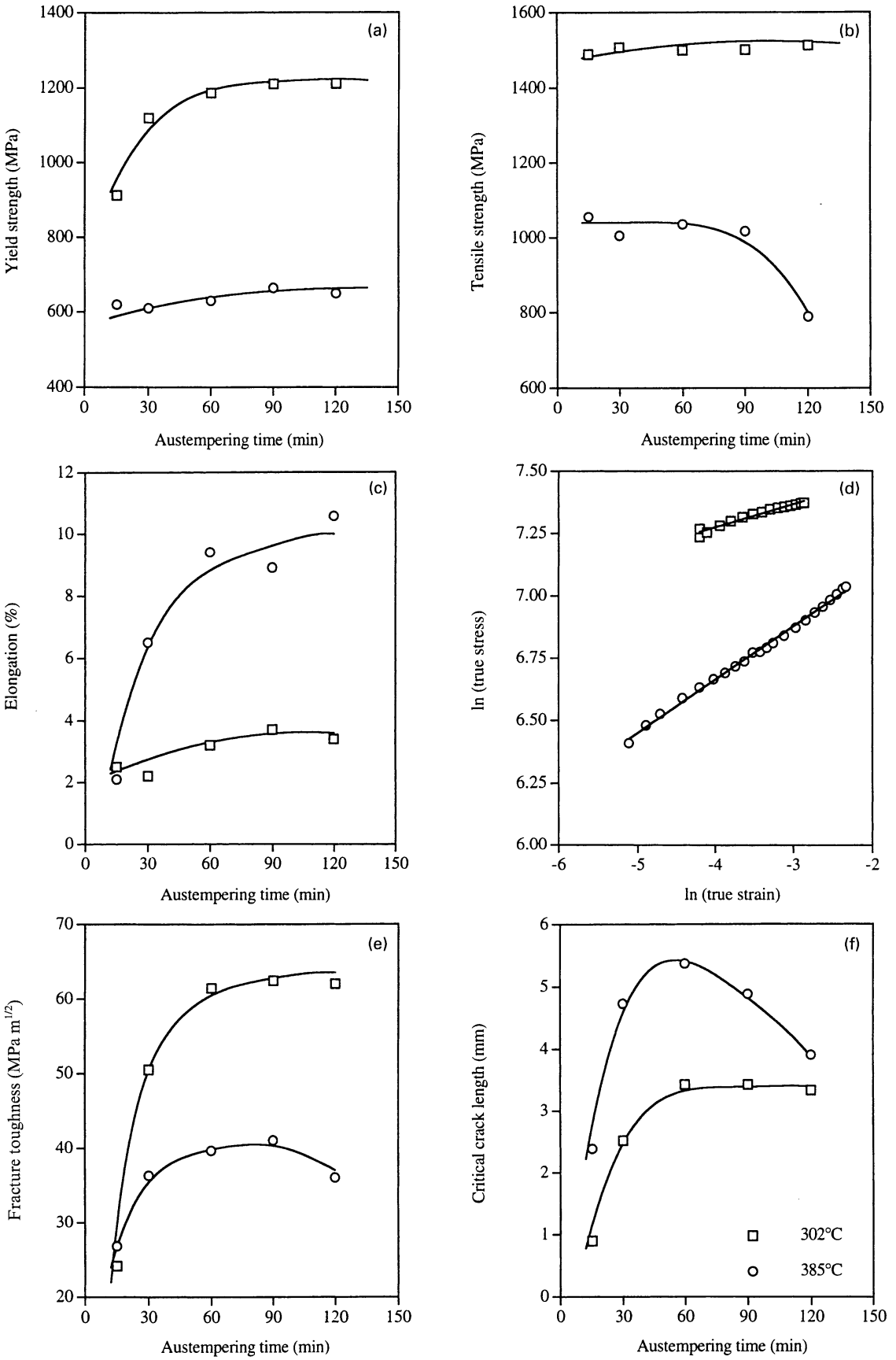

a yield strength *v.* austempering time; *b* tensile strength *v.* austempering time; *c* elongation *v.* austempering time; *d* logarithmic true stress *v.* true strain; *e* fracture toughness *v.* austempering time; *f* critical crack length *v.* austempering time

4 Mechanical property relationships of austempered specimens

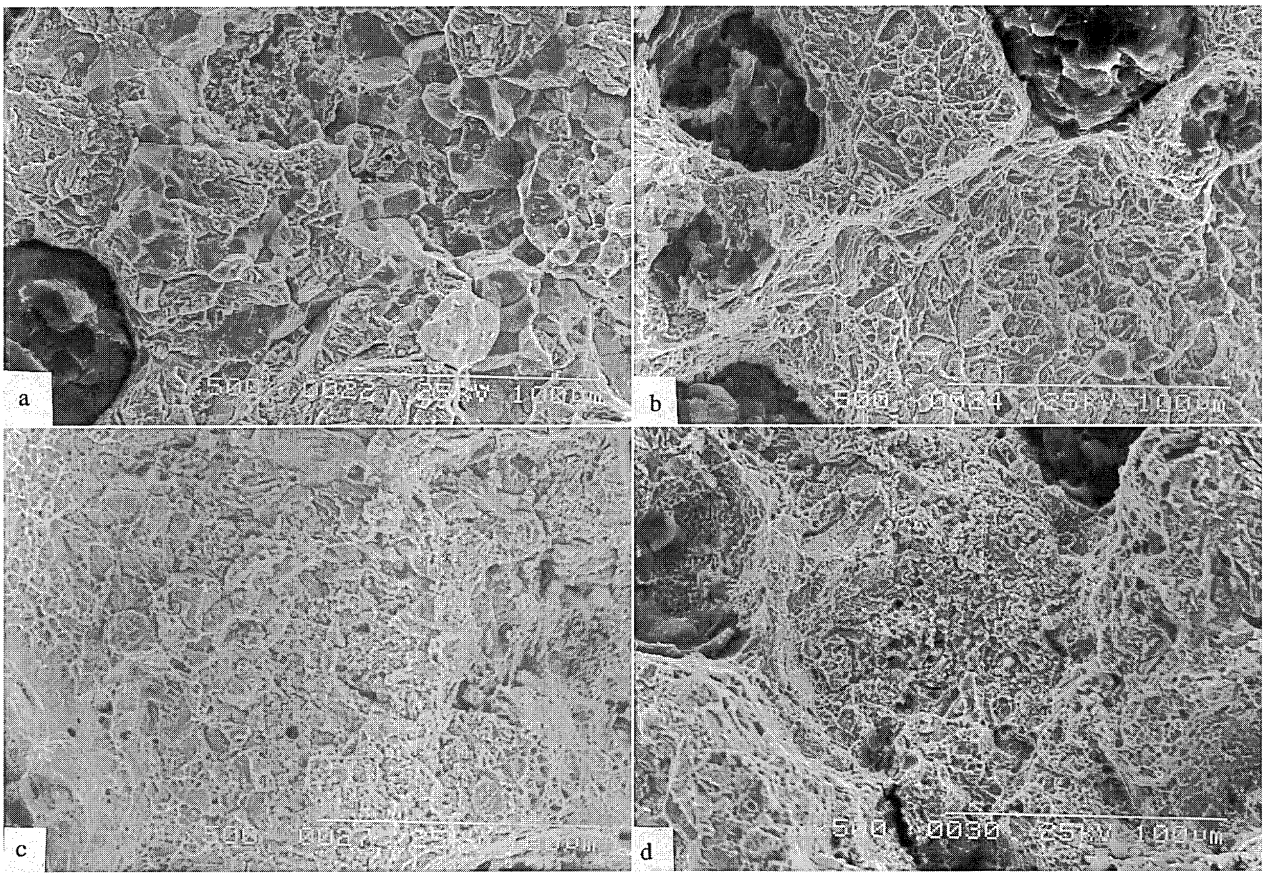

a 15 min; *b* 30 min; *c* 60 min; *d* 90 min

5 Fractographs of fracture toughness specimens austempered at 302°C for given times

very low fracture toughness. The fracture mode changed to the transgranular type at both temperatures after 30 min (Figs. 5*b* and 6*b*). Beyond half an hour, entirely different fracture modes were observed at the two temperatures. When austempered for 60 min or longer at 302°C predominantly dimpled ductile fracture was observed. However, at 385°C the fracture mode continued to be transgranular cleavage even at the longest duration (120 min) employed in this work (Figs. 6*c* and *d*). It should be noted that the corresponding tensile specimens showed highly ductile fracture. Thus the fracture appearance reflects the fracture toughness of the material.

Austempered ductile iron with a lower ausferrite microstructure showed high tensile strength and low ductility. With relatively low tensile toughness, it had high fracture toughness. However, ADI with an upper ausferrite microstructure exhibited low tensile strength and high ductility, but low fracture toughness. A possible reason may be carbide precipitation at high austempering temperatures.[33] This was noted in specimens austempered for 2 h at 385°C because of the small dip in carbon content shown in Fig. 3*b*. However, it does not explain the low fracture toughness of specimens austempered for 30 and 60 min, both of which had a high retained austenite content and also high carbon content in the austenite.

A second possible mechanism for the low fracture toughness is the formation of martensite owing to the thermal instability of austenite. But at the high level of carbon content of these austenites, M_s temperatures have been estimated to be in the region of -150 to -200°C. Therefore formation of martensite is very unlikely, unless there is considerable non-uniformity in the composition of the austenite. Since carbon has to diffuse into austenite from regions transforming to ferrite, complete diffusion to the centre of the austenite region may not occur if the diffusion distances are long. Thus austenite regions may have higher carbon near the ferrite interface, and lower carbon at the centre. The centre may transform to martensite, and being brittle, provide an easy path for crack propagation. However, using the diffusion coefficient of carbon in austenite as $D = 1 \times 10^{-5} \exp(-136\,000/RT)\ \mathrm{m^2\ s^{-1}}$ (Ref. 34) and root mean square diffusion distance as $x = (4Dt)^{1/2}$, x is calculated to be 2 μm at $t = 2$ h and $T = 385$°C. This is of the same magnitude as the distance between the ferrite blade and the centre of the austenite region. Thus it is reasonable to assume that the austenite has a uniform composition. Martensite formation owing to the thermal instability of the austenite can be ruled out as a possible cause of low fracture toughness. Formation of stress induced martensite is another possibility that deserves consideration. But such a transformation would be expected to increase toughness through the transformation induced plasticity (TRIP) phenomenon,[17,35–36] rather than decrease it as observed in the present work. Also, metallographic examination through optical microscopy and SEM did not reveal the presence of any martensite along the edge of the fracture surface. Therefore the phenomenon of stress induced martensite formation can also be ruled out in the present case.

In bainitic steels also it is generally found that lower bainitic microstructures give better toughness than upper bainitic microstructures. Johnson and Becker[37] attributed this to the presence of large carbides, whose cracking and debonding along the ferrite carbide interface was responsible for the lower toughness of the upper bainitic microstructure. This cannot be valid for ADI since no carbide precipitation is observed if austempered within optimum limits. Also, smaller bainitic packet sizes result in smaller cleavage facet length.[38] The smaller the cleavage facet, the more frequent the high energy tear fracture will be, and the higher the

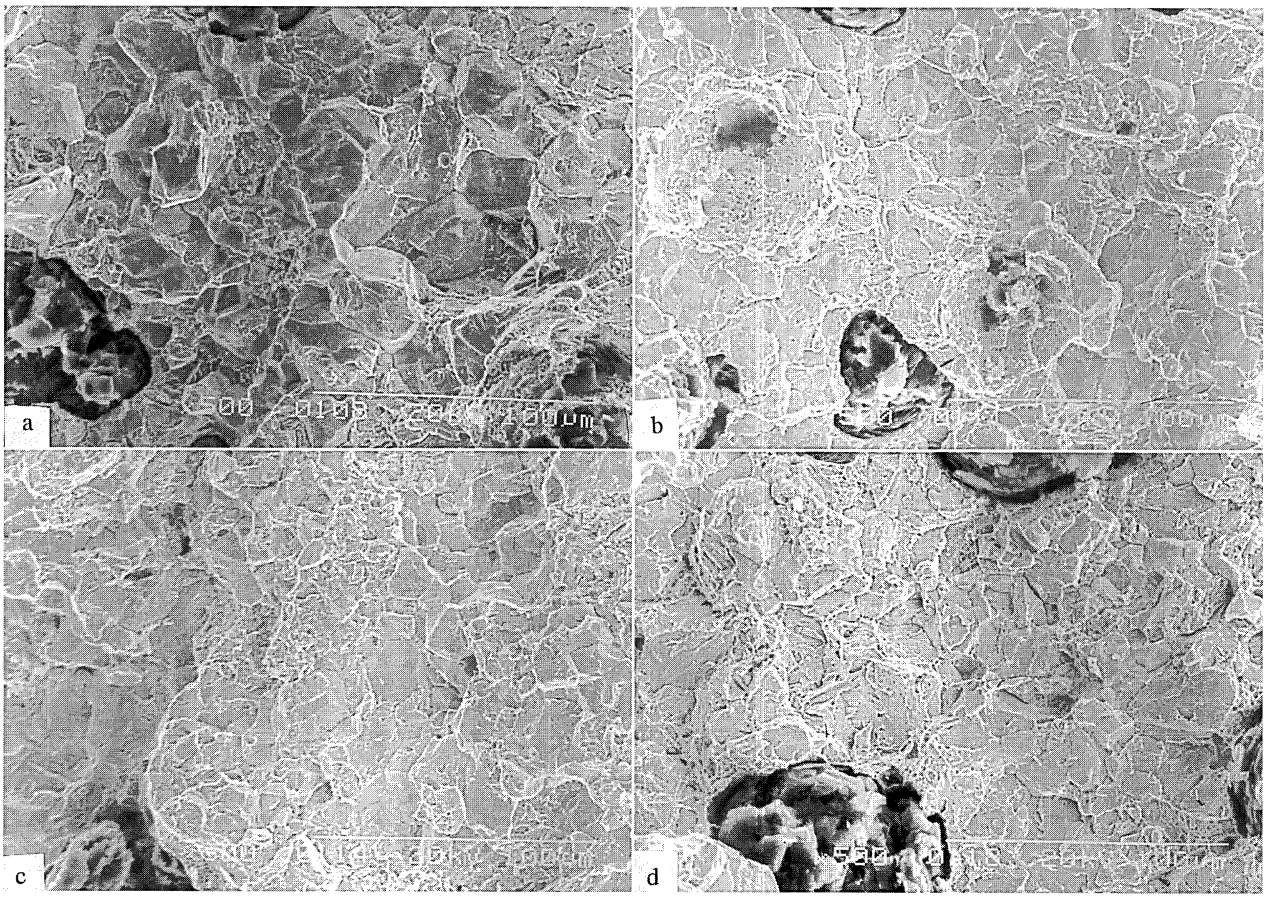

a 15 min; *b* 30 min; *c* 60 min; *d* 90 min

6 Fractographs of fracture toughness specimens austempered at 385°C for given times

fracture toughness will be. This argument is not wholly acceptable in ADI because the packet consists of ferrite and austenite. Therefore, in lower ausferrite structures a thin layer of austenite separates the ferrite laths. Hence the packet cannot be treated as a single unit. Also, increasing austempering temperature gives increasing prior austenite grain size. This should increase the packet size, and therefore, should decrease toughness. However, reports[14,21] indicate that at 850 to 920°C, increasing austempering temperature increases fracture toughness.

The results of a study of microstructural aspects of fracture in austempered ductile iron by Voigt *et al.*[39] are relevant to the present investigation in interpreting the fracture mechanism. They showed that crack initiation and propagation can be divided into several distinct microstructural events. Initially there was decohesion at the graphite/matrix interface well ahead of the propagating crack. This was followed by plastic deformation in the matrix, primarily concentrated in ferrite laths. Continued plastic deformation resulted in initiation of microcracks. These joined up to form a larger crack, which eventually joined up with the main crack. The microcracks started primarily within the ferrite or at the ferrite/austenite interface, and selected a localised path of least resistance, avoiding travelling through regions of stabilised austenite as far as possible. Often the microcracks were temporarily blunted by regions of austenite. Very similar events were observed in specimens austempered at 400 or at 300°C.

Thus it is very clear that the crack initiation and propagation is controlled by the microstructural constituents, namely graphite nodules, ferrite, and austenite. The size, density, and distribution of graphite nodules are very important factors with a significant influence on fracture toughness. In the present work, however, these can be ignored, since they have not been used as variables. By changing the austempering time and temperature, the amount of ferrite and its morphology have been varied. Therefore, the variation in fracture toughness should reflect the variation in these microstructural constituents.

The critical amount of work required to initiate an unstable fracture is given as[40]

$$G_{1C} = 2\sigma_y V_C^* \quad \ldots\ldots\ldots\ldots\ldots\ldots (6)$$

where $2V_C^*$ is the critical value of the crack opening displacement and σ_y is the yield strength of the material. We further have[40]

$$K_{1C}^2 = \frac{EG_{1C}}{1-\nu^2} = \frac{2E\sigma_y V_C^*}{1-\nu^2} \quad \ldots\ldots\ldots\ldots\ldots\ldots (7)$$

where E is Young's modulus and ν is Poisson's ratio.

We can write[40]

$$2V_C^* = 2\rho\varepsilon_f \quad \ldots\ldots\ldots\ldots\ldots\ldots (8)$$

where ρ is the crack tip radius and ε_f is the fracture strain of the material. Substituting (8) in (7)

$$K_{1C}^2 = \frac{2E\rho\varepsilon_f\sigma_y}{1-\nu^2} \quad \ldots\ldots\ldots\ldots\ldots\ldots (9)$$

Strain at fracture ε_f depends on the microstructure. A comparison of Figs. 3*a* and 4*c* shows that strain at fracture increases with retained austenite content. Besides austenite content, strain hardening ability is also an important factor in influencing ε_f through its effect on uniform elongation ε_u. Several investigators[41–44] have shown that high strain hardening in high carbon austenitic steels is a result of interaction between dislocations and carbon atoms. It has been shown[45] using TEM that ADI microstructures contain

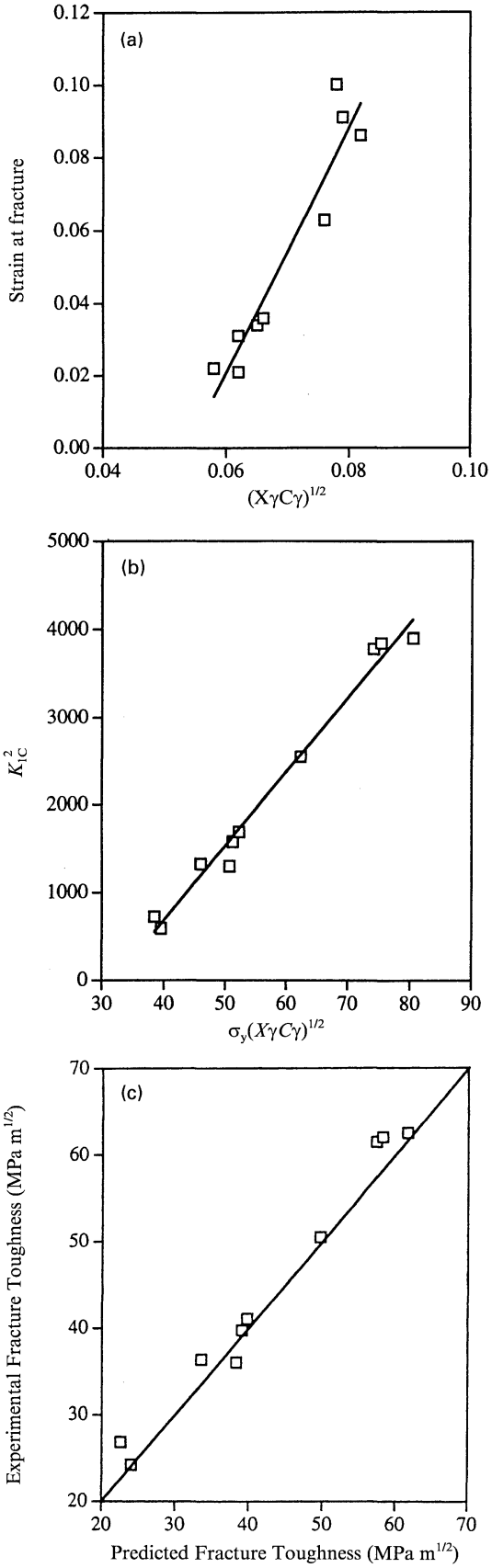

7 Plot of *a* strain at fracture versus $(X_\gamma C_\gamma)^{1/2}$; *b* K_{1C}^2 versus $\sigma_y(X_\gamma C_\gamma)^{1/2}$; and *c* experimental values of fracture toughness versus predicted values

heavy dislocation densities. It has also been shown[46] that dynamic strain aging occurs in ADI over a wide temperature range. Therefore it is quite conceivable that interactions do exist between dislocations and carbon atoms. Increasing the carbon content of the austenite will therefore increase the strain hardening and the uniform strain ε_u. The parameter $X_\gamma C_\gamma$ is therefore of special significance. This parameter is recognised[4] as representing the total carbon in the retained austenite. Figure 4*d* shows that strain hardening increases as the austempering temperature is increased from 302 to 385°C. The former corresponds to an $X_\gamma C_\gamma$ value of 0·39 while the latter corresponds to 0·67. We can, therefore, write

$$\varepsilon_u \propto (X_\gamma C_\gamma)^a \quad \ldots\ldots\ldots\ldots\ldots\ldots \quad (10)$$

where a is a constant. Because of the size difference, a carbon atom in solid solution in iron will produce a misfit strain field which may interact with the dislocation strain field. Analysis of the strain field–dislocation interaction[47,48] gives an expression for solution hardening that is proportional to the square root of the solute concentration. Experiments generally show reasonable agreement with this prediction.[48,49] The value of the constant a in equation (10) is therefore taken to be 1/2. In the present investigation all the specimens, whether austempered at 302 or at 385°C, failed without necking in tensile tests. The fracture strain is therefore the same as the uniform elongation at fracture. A plot of the strain at fracture against $(X_\gamma C_\gamma)^{1/2}$ results in a straight line as shown in Fig. 7*a*. Therefore

$$\varepsilon_f = C_1(X_\gamma C_\gamma)^{1/2} + C_2 \quad \ldots\ldots\ldots\ldots \quad (11)$$

where C_1 and C_2 are constants estimated to be 3·36 and −0·182 respectively from the plot. The plot also suggests that when $X_\gamma C_\gamma$ is below $2{\cdot}7 \times 10^{-3}$, ductility will be zero.

Substituting (11) in (9)

$$K_{1C}^2 = \frac{2E\rho C_1}{1-\nu^2}\sigma_y(X_\gamma C_\gamma)^{1/2} + \frac{2E\rho}{1-\nu^2}C_2\sigma_y \quad \ldots\ldots \quad (12)$$

The second term in the above equation should be the value of K_{1C}^2 when $(X_\gamma C_\gamma)$ is zero. However, the equation predicts zero fracture toughness at the $X_\gamma C_\gamma$ value of $2{\cdot}7 \times 10^{-3}$ (the same value for which ε_f is zero). Therefore, the second term is taken as a constant with $\sigma_y = 610$ MPa, the minimum yield strength in the present investigation. The above equation, then, predicts a linear relationship between K_{1C}^2 and $\sigma_y(X_\gamma C_\gamma)^{1/2}$. Linear regression analysis by the method of least squares resulted in a straight line as shown in Fig. 7*b*. The correlation coefficient is 0·993.

Taking E as 207 GPa (Ref. 31), ν as 0·3 and a reasonable value of 50 μm for ρ, we can rewrite equation (12) as

$$K_{1C}^2 = 78{\cdot}6\sigma_y(X_\gamma C_\gamma)^{1/2} - 2524 \quad \ldots\ldots\ldots\ldots \quad (13)$$

The constants in the above equation match well with the slope of 84·9 and the y intercept of −2714 for the straight line in Fig. 7*b*. Fracture toughness values were calculated for all the heat treatment conditions of the present investigation using equation (13). These are plotted against the experimental values in Fig. 7*c*. The points lie very close to the 45° line showing very good agreement between the experimental and predicted values.

According to equation (13), fracture toughness is dependent on yield strength and volume fraction of retained austenite and its carbon content. Increasing each of these to the maximum possible value will therefore maximise fracture toughness. Values of these parameters depend on austempering temperature. The parameter $X_\gamma C_\gamma$, which is a measure of the total carbon in the retained austenite, increases with increasing austempering temperature, because of the increasing diffusion of carbon. Even though C_γ decreases with increasing temperature, the large increase in X_γ more than compensates for it. In the present investigation, the parameter $X_\gamma C_\gamma$ was found to be 0·44 wt-% at 302°C and 0·64 wt-% at 385°C. In a previous

investigation[50] it has been reported that $X_\gamma C_\gamma$ values were 0·32, 0·35, 0·41, 0·47, 0·64, and 0·63 wt-% at austempering temperatures of 260, 288, 302, 316, 357, and 385°C respectively. It can therefore be concluded that $X_\gamma C_\gamma$ increases with increasing austempering temperature. But the yield strength decreases as austempering temperature increases. It is thus not possible to maximise σ_y and $X_\gamma C_\gamma$ simultaneously. At an intermediate temperature, both σ_y and $X_\gamma C_\gamma$ will have moderately high values, resulting in high fracture toughness. As the austempering temperature is increased, the fracture toughness will initially increase, reach a maximum, and then drop, as reported by several investigators.[18–21]

It has been reported that yield strength depends on the fineness of the ferrite blades. Harrynen *et al.*,[51] and Ali *et al.*[52] have shown that the yield strength of ADI can be expressed as

$$\sigma_y = \sigma_0 + Ad^{-1/2} + BX_\gamma \quad . \quad . \quad . \quad . \quad . \quad . \quad . \quad . \quad . \quad . \quad (14)$$

where d is the ferrite particle size, X_γ is the volume fraction of austenite and σ_0, A, and B are constants. Both studies[51,52] have shown that A is much larger than B. The yield strength of ADI is primarily decided by the ferrite particle size. Substituting (14) into (13) we can see that K_{1C}^2 varies with $(X_\gamma C_\gamma/d)^{1/2}$. From the microstructural point of view, fracture toughness can be maximised by austempering in such a way as to get very fine ferrite, high austenite content, and as much carbon as possible in the austenite.

Conclusions

1. Austempered ductile iron (ADI) with lower ausferrite microstructure has higher fracture toughness than ADI with upper ausferrite microstructure.
2. Austempered ductile iron with upper ausferrite microstructure has a higher tensile toughness and strain hardening coefficient. The latter is related to its high retained austenite content and the high carbon content of the retained austenite.
3. It is found that K_{1C}^2 is directly proportional to $\sigma_y(X_\gamma C_\gamma)^{1/2}$. The fracture toughness of ADI can be maximised by maximising σ_y, X_γ, and C_γ.
4. Since $X_\gamma C_\gamma$ increases with austempering temperature, and σ_y decreases, maximum fracture toughness will be attained at an intermediate temperature. Fracture toughness will go through a maximum as the austempering temperature is increased.

Acknowledgement

This work was financially supported by the Ford Motor Co., Dearborn, MI, USA.

References

1. M. JOHANSSON: *AFS Trans.*, 1977, **85**, 117.
2. J. DODD: *Mod. Cast.*, 1978, **68**, 60.
3. R. B. GUNDALACH and J. F. JANOWAK: *AFS Trans.*, 1983, **91**, 377.
4. T. N. ROUNS, K. B. RUNDMAN, and D. M. MOORE: *AFS Trans.*, 1984, **92**, 815.
5. R. A. HARDING and G. N. J. GILBERT: *Br. Foundryman*, 1986, **79**, 489.
6. D J. MOORE, T. N. ROUNS, and K. B. RUNDMAN: *AFS Trans.*, 1985, **93**, 705.
7. R. B. GUNDALACH and J. F. JANOWAK: *Met. Prog.*, 1985, **128**, 19.
8. R. GUNDALACH and J. JANOWAK: in Proc. 2nd Int. Conf. on 'Austempered ductile iron', Ann Arbor, MI, USA, March 1986, ASME Gear Research Institute, 23.
9. S. M. SHAH and J. D. VERHOEVEN: *Wear*, 1986, **113**, 267.
10. I. SCHMIDT and A. SCHUCHERT: *S. Metallkd.*, 1987, **78**, 871.
11. L. BARTOSIEWICZ, A. R. KRAUSE, F. A. ALBERTS, I. SINGH, and S. K. PUTATUNDA: *Mater. Charact.*, 1993, **30**, 221.
12. P. SHANMUGAM, P. P. RAO, K. R. UDUPA, and N. VENKATARAMAN: *J. Mater. Sci.*, 1994, **29**, 4933.
13. P. P. RAO and P. PADMAPRABHA: *Fatigue Fract. Eng. Mater. Struct.*, 1995, **18**, 693.
14. K. ZUM GHAR and B. L. WAGNER: *Arch. Eisenhüttenwes.*, 1979, **50**, 269.
15. G. BARBEZAT and H. MAYER: *Sulzer Tech. Rev.*, 1986, **2**, 32.
16. S. C. LEE and C. C. LEE: *AFS Trans.*, 1988, **96**, 827.
17. J. ARANZABAL, I. GUTIERREZ, J. M. RODRIGUEZ-IBABE, and J. J. URCOLA: *Mater. Sci. Technol.*, 1992, **8**, 263.
18. L. BARTOSIEWICZ, I. SINGH, F. A. ALBERTS, A. R. KRAUSE, and S. K. PUTATUNDA: *J. Mater. Eng. Perform.*, 1995, **4**, 90.
19. S. K. PUTATUNDA and I. SINGH: *J. Test. Eval.*, 1995, **23**, 325.
20. J. L. DOONG, F. C. JU, H. S. CHEN, and L. W. CHEN: *J. Mater. Sci. Lett.*, 1986, **5**, 555.
21. J. L. DOONG and C. S. CHEN: *Fatigue Fract. Eng. Mater. Struct.*, 1989, **12**, 155.
22. M. GRECH, P. BOWEN, and J. M. YOUNG: in Proc. World Conf. on 'Austempered ductile iron', Bloomingdale, IL, USA, March 1991, American Foundrymen's Society, 338.
23. R. C. KLUG, M. B. HINTZ, and K. B. RUNDMAN: *Metall. Trans. A*, 1985, **16A**, 797.
24. K. B. RUNDMAN and R. C. KLUG: *AFS Trans.*, 1982, **90**, 499.
25. B. D. CULLITY: 'Elements of X-ray diffraction', 411; 1974, Reading, MA, Addison-Wesley.
26. C. S. ROBERTS: *Trans. AIME*, 1953, **197**, 203.
27. 'Annual book of ASTM Standards', Vol. 03.01, 130; 1992, Philadelphia, PA, ASTM.
28. 'Annual book of ASTM Standards', Vol. 03.01, 745; 1992, Philadelphia, PA, ASTM.
29. T. N. ROUNS and K. B. RUNDMAN: *AFS Trans.*, 1988, **96**, 851.
30. R. C. VOIGT and C. R. LOPER: in Proc. 1st Int. Conf. 'Austempered ductile iron', Metals Park, OH, USA, American Society for Metals, April 1984, 83.
31. G. E. DIETER: 'Mechanical metallurgy'; 1986, New York, McGraw-Hill.
32. T. H. HOLLOMON: *Trans. AIME*, 1945, **162**, 268.
33. L. SIDJANIN and R. E. SMALLMAN: *Mater. Sci. Technol.*, 1992, **8**, 1095.
34. E. A. BRANDES (ed.): 'Smithells metals reference book', 6th edn; 1983, London, Butterworths.
35. E. DORAZIL and M. HOLZMANN: in Proc. World Conf. on 'Austempered ductile iron', Bloomingdale, IL, USA, March 1991, American Foundrymen's Society, 32.
36. T. KOBAYASHI, H. YAMAMOTO, and S. YAMADA: in Proc. World Conf. on 'Austempered ductile iron', Bloomingdale, IL, USA, March 1991, American Foundrymen's Society, 567.
37. D. R. JOHNSON and W. T. BECKER; *J. Mater. Eng. Perform.*, 1993, **2**, 255.
38. Y. TOMITA and K. OKABAYASHI: *Metall. Trans. A*, 1986, **17A**, 1203.
39. R. VOIGT, H. DHANE, and L. ELDOKY: in Proc. 2nd Int. Conf. on 'Austempered ductile iron', Ann Arbor, MI, USA, March 1986, ASME Gear Research Institute, 327.
40. A. S. TETELMAN and A. J. MCEVILY: 'Fracture of structural materials', 1967, New York, Wiley.
41. C. H. WHITE and R. W. K. HONEYCOMBE: *J. Iron Steel Inst.*, 1962, **200**, 457.
42. W. N. ROBERTS: *Trans. AIME*, 1964, **230**, 373.
43. Y. N. DASTUR and W. C. LESLIE: *Metall. Trans. A*, 1981, **12A**, 749.
44. P. H. ADLER, G. B. OLSON, and W. S. OWEN: *Metall. Trans. A*, 1986, **17A**, 1725.
45. V. FRANETOVIC, M. M. SHEA, and E. F. RYNTZ: *Mater. Sci. Eng.*, 1987, **96**, 231.
46. C. S. SHIEH, T. S. LUI, and L. H. CHEN: *Mater. Trans., JIM*, 1995, **36**, 620.
47. P. M. KELLY: *J. Aust. Inst. Metals*, 1971, **16**, 104.
48. M. Z. BUTT and P. FELTHAM: *J. Mater. Sci.*, 1993, **28**, 2557.
49. D. PECKNER: 'The strengthening of metals'; 1964, New York, Reinhold.
50. P. P. RAO and S. K. PUTATUNDA: *Metall. Mater. Trans. A*, 1997, **28A**, 1457.
51. K. L. HARRYNEN, D. J. MOORE, and K. B. RUNDMAN: *AFS Trans.*, 1990, **98**, 471.
52. A. S. H. ALI, K. I. UZLOV, N. DARWISH, and R. ELLIOT: *Mater. Sci. Eng.*, 1994, **10**, 35.